

Isobaric Analog Resonances in Proton Elastic Scattering from $^{136}\text{Xe}^\dagger$

P. A. MOORE* AND P. J. RILEY†

University of Texas, Austin, Texas

AND

C. M. JONES AND M. D. MANCUSI‡

Oak Ridge National Laboratory, Oak Ridge, Tennessee 37830

AND

J. L. FOSTER, JR.

University of Pittsburgh, Pittsburgh, Pennsylvania

(Received 12 November 1968)

Isobaric analog states have been observed in proton elastic scattering from ^{136}Xe at proton energies from 9.77 to 12.98 MeV. The observed levels in ^{137}Cs are identified as analogs of low-lying states of ^{137}Xe . The data have been analyzed using a shell-model description of isobaric analog resonances. Orbital angular momentum transfer values, resonance energies, total and partial widths, and spectroscopic factors for most of the observed resonances are presented. The spectroscopic factors are shown to be highly insensitive to the choice of optical-model parameters. The results are compared with (d , p) studies on the target nucleus. The observed Coulomb displacement energy is 14.057 ± 0.040 MeV.

I. INTRODUCTION

IN recent years, isobaric analog resonances have been shown to provide a useful tool for the study of nuclear structure in heavy nuclei. In the closed $N=82$ neutron shell, analog resonances have been studied through proton elastic scattering from ^{138}Ba , ^{140}Ce , ^{142}Nd , and ^{144}Sm ,¹ and a comparison with similar measurements on ^{136}Xe is of interest. The use of ^{136}Xe as a target offers, in addition, an advantage in that a gaseous target allows accurate absolute cross-section measurements. Further, since, xenon until recently, has been difficult to obtain with high isotopic purity, few experimental measurements have been carried out with the xenon isotopes.

Elastic scattering measurements at isobaric analog resonances yield information similar to that obtained from (d , p) studies on the target nucleus, where one measures the overlap between final states and the state composed of a single neutron coupled to the ground state of the target. In the present case, the parent analog states in ^{137}Xe can be expressed as

$$\Psi_{\text{PA}}^m(^{137}\text{Xe}) = \sum_{k, l_j} b_{km}^{l_j} [\varphi_c^{k\nu}(l_j)],$$

where $\varphi_c^{k\nu}$ denotes the orthonormal set of ^{136}Xe states, with φ_c^0 being the ground state, and $\nu(l_j)$ denotes the neutron states. Ψ_{PA}^m is often referred to as the $n\text{C}$ system. The $T_>$ part of the analog resonance, obtained

through the T^- operator acting on the parent analog system, is expressed by

$$\Psi_{\text{A}}^m(^{137}\text{Cs}) = \sum_{k, l_j} [b_{km}^{l_j} / (2T_0 + 1)^{1/2}] \times [\varphi_c^{k\nu}(l_j) + (2T_0)^{1/2} (T^- \varphi_c^{k\nu})(l_j)],$$

where $\pi(l_j)$ indicates the single-proton state. The elastic-proton partial width can be expressed by

$$\Gamma_0^{l_j} \propto (b_{0m}^{l_j})^2 / (2T_0 + 1).$$

Consequently, at analog resonances, the elastic proton width is expected to be simply related to the spectroscopic factor of the corresponding analog state. A method has recently been developed² for quantitative extraction of spectroscopic factors using the shell-model description of isobaric analog resonances of Mahaux and Weidenmüller.³ This method has been used for the analysis of the present data. Comparisons have been made with the low-lying parent levels in ^{137}Xe studied in (d , p) measurements on the same target.^{4,5}

II. EXPERIMENTAL PROCEDURE

The incident proton beam was obtained from the Oak Ridge National Laboratory EN Tandem Van de Graaff accelerator. The target gas, isotopically enriched to 91% ^{136}Xe and 8% ^{134}Xe , was contained within a 3-in.-diam gas cell used in conjunction with the ORNL precision gaseous target scattering chamber.⁶ Beam entrance and exit windows were 25- μm -thick nickel foils. The cell walls were 0.00025-in.-thick aluminized

² S. A. A. Zaidi and S. Darmodjo, *Phys. Rev. Letters* **19**, 1446 (1967).

³ C. Mahaux and H. A. Weidenmüller, *Nucl. Phys.* **89**, 33 (1966); H. A. Weidenmüller, *Nucl. Phys.* **A99**, 269 (1967); **A99**, 289 (1967).

⁴ E. J. Schneid and B. Rosner, *Phys. Rev.* **148**, 1241 (1966).

⁵ P. A. Moore, P. J. Riley, C. M. Jones, M. D. Mancusi, and J. L. Foster, Jr., *Phys. Rev.* **175**, 1516 (1968).

⁶ C. M. Jones, J. W. Johnson, and R. M. Beckers, *Nucl. Instr. Methods* **68**, 70 (1969).

† Research sponsored by the U.S. Atomic Energy Commission under contract with Union Carbide Corp.

* Research participation at Oak Ridge National Laboratory sponsored by Oak Ridge Associated Universities.

‡ U.S. Atomic Energy Commission Postdoctoral Fellow under appointment from the Oak Ridge Associated Universities. Present address: Bell Telephone Laboratories, Holmdel, N.J.

¹ P. von Brentano, N. Marquardt, J. P. Wurm, and S. A. A. Zaidi, *Phys. Letters* **17**, 124 (1965); G. C. Morrison, *Bull. Am. Phys. Soc.* **12**, 8 (1967); J. P. Wurm, P. von Brentano, E. Grosse, H. Seitz, C. A. Wiedner, and S. A. A. Zaidi, in *Isobaric Spin in Nuclear Physics*, edited by J. D. Fox and D. Robson (Academic Press Inc., New York, 1966), p. 790; J. L. Foster, O. Dietzsch, and K. Schechet, *Bull. Am. Phys. Soc.* **13**, 70 (1968).

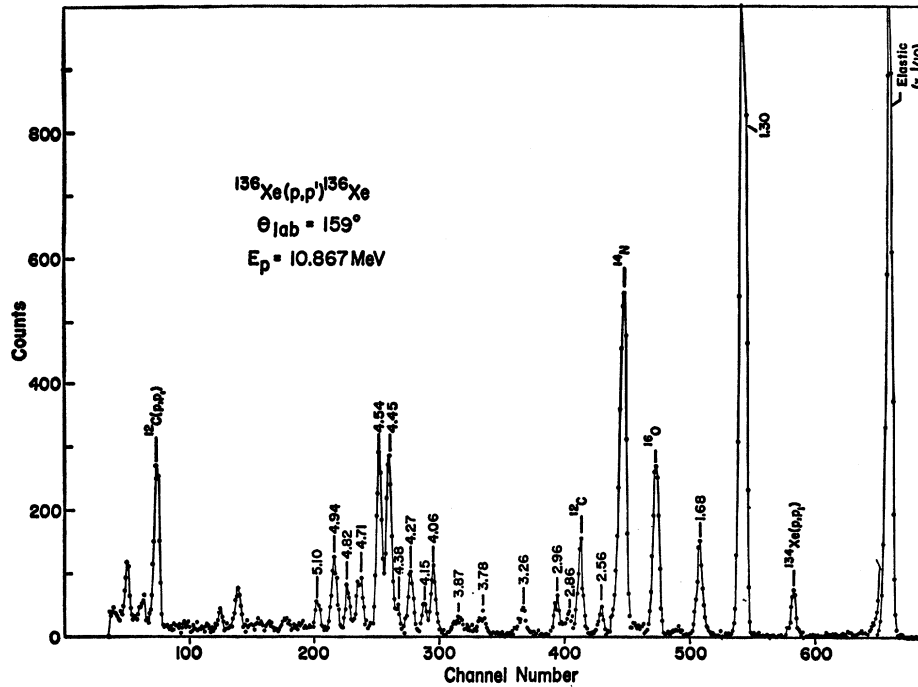


FIG. 1. Typical pulse-height spectrum for the scattering of protons from ^{136}Xe at a scattering angle of 159.0° and a laboratory proton energy of 10.874 MeV. The excitation of states seen in ^{136}Xe through proton inelastic scattering are indicated on the figure.

Mylar. The beam current used was typically $0.3 \mu\text{A}$, and the total charge collection at each energy was approximately $400 \mu\text{C}$. The gas pressure was typically 0.068 atm, corresponding to a target thickness of approximately $(250/\sin\theta_{\text{lab}}) \mu\text{g}/\text{cm}^2$. Four 2-mm-thick lithium-drifted silicon detectors, cooled to dry-ice temperature, were used. A typical pulse-height spectrum, measured for a beam energy of 10.874 MeV at a laboratory angle of 159.0° , is shown in Fig. 1. Slight contamination was present, as the spectrum indicates,

and is attributed to oxygen, nitrogen, and carbon. The over-all experimental uncertainty in the measured absolute cross sections is of the order of $\pm 4\%$ (standard deviation). The over-all experimental resolution was 50 keV.

Excitation functions for the scattering of protons from ^{136}Xe were measured for proton energies between 9.77 and 12.98 MeV at laboratory angles of 90.0° , 123.75° , 146.25° , and 159.0° . The beam energy was calibrated using the $^{27}\text{Al}(p, n)$ threshold, and is believed to have an uncertainty of ± 20 keV (standard deviation). Initially, excitation functions were measured from 9.767 to 12.537 MeV; later, these measurements were extended from 11.530 to 12.976 MeV. The elastic scattering data is shown in Fig. 2. The overlapping region indicates good reproducibility of data measured on two separate occasions. The elastic scattering cross sections were not corrected for the 8% ^{134}Xe contamination, so that the reported cross sections are actually those for 91% ^{136}Xe and 8% ^{134}Xe .

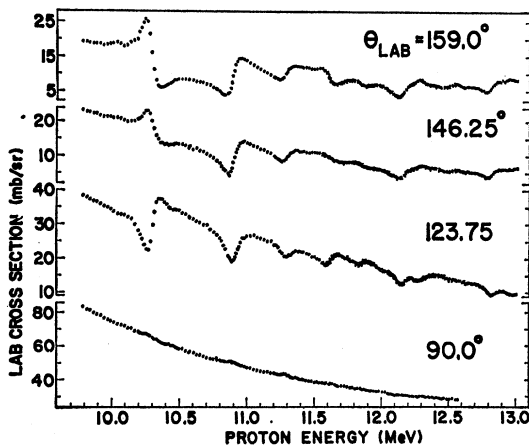


FIG. 2. Excitation functions for the elastic scattering of protons from ^{136}Xe at laboratory angles of 90.0° , 123.75° , 146.25° , and 159.0° for laboratory proton energies from 9.77 to 12.98 MeV. Circles and crosses indicate data measured at different times. Statistical and relative experimental uncertainties are smaller than the data points. The data shown on this figure and on Figs. 3, 4, and 6 are the observed cross sections for an isotopic mixture of 91% ^{136}Xe and 8% ^{134}Xe .

III. THEORETICAL ANALYSIS

Following Mahaux and Weidenmüller,³ the energy averaged scattering matrix for elastic scattering on spin-zero targets is given by

$$\langle S_{l_i} \rangle = \exp(2i\delta_{l_i}) - i \exp(2i\alpha_{l_i}) [\Gamma_{l_i} / (E - E_R + \frac{1}{2}i\Gamma)], \quad (1)$$

where

$$\Gamma_{l_i} = \Gamma_{l_i}^{(\Lambda)} \left[\frac{1 + 2iY_{l_i}(\Delta_{l_i}/P_{l_i})}{1 + Y_{l_i}} \right]^2 \quad (2)$$

and

$$\exp(2i\delta_{l_i}) = 2i\alpha_{l_i}[(1 - Y_{l_i})/(1 + Y_{l_i})]. \quad (3)$$

δ_{l_i} is the optical-model phase shift for the pC system, and α_{l_i} is its real part. Δ_{l_i} is the energy shift due to the decay of a proton from an isobaric analog resonance. Γ_{l_i} is the width of the single-particle resonances displayed by solutions of the equation

$$[k + U_0 + V_c + \frac{1}{2}T_0V_1 - E_p]\chi_{\text{pC}} = 0. \quad (4)$$

All other quantities are defined in Ref. 3.

In the present analysis, code JULIUS⁷ was used to generate theoretical elastic scattering excitation functions using expressions (1)–(3) for the scattering matrix. The code uses a potential with a surface-peaked imaginary part and a real spin-orbit part:

$$\begin{aligned} V(r) = & -Vf(r, r_0, a_r) && \text{(central)} \\ & -iAa_iW_D(d/dr)f(r, r_0, a_i) \\ & + \delta \cdot 1V_{\text{so}}(\hbar/m\pi c)^2 r^{-1}(d/dr)f(r, r_0, a_r) && \text{(spin orbit)} \\ & + \begin{pmatrix} (Ze^2/2r_c)(3 - r^2/r_c^2) & \text{if } r \leq r_c \\ Ze^2/r & \text{if } r < r_c \end{pmatrix}. && \text{(C)} \end{aligned}$$

The function $f(r, r_0, a)$ is the usual Saxon-Woods shape

$$f(r, r_0, a) = \{1 + \exp[-(r - r_0)A^{1/3}/a]\}^{-1}.$$

Zaidi and Darmodjo² showed that the theoretical proton partial width of an analog resonance can be calculated from the expression

$$\Gamma_{l_i}(\text{theor}) = (kT_0/E) |\langle \varphi_{\text{nA}} | V_1 | \chi_{\text{pC}}^{(+)} \rangle|^2.$$

The radial wave functions φ_{nA} and $\chi_{\text{pC}}^{(+)}$ are obtained by numerical integration of the homogeneous part of the Lane equations. The potentials binding the parent analog states, used in the calculation of φ_{nA} , and the real part of the proton optical-model potential for the pC system, used in the calculation of $\chi_{\text{pC}}^{(+)}$, are related through the equation

$$T_0V_1(r) + V_p(r) = V_n(r),$$

where

$$\frac{1}{2}(T_0V_1) = 26(N - Z)/A,$$

in agreement with the value obtained from analysis of charge-exchange (p, n) reactions.⁸ A real volume-type charge-exchange potential

$$V_1(r) = V_1\{1 + \exp[-(r - r_0)A^{1/3}/a]\}^{-1}$$

was used. The spectroscopic factor of the analog state is then given by

$$S_{pp} = \Gamma_{l_i}^{(\text{A})}/\Gamma_{l_i}(\text{theor}).$$

Code GPMAIN,⁷ a modified version of the bound-state

⁷ S. A. A. Zaidi (private communication); S. Darmodjo, dissertation, University of Texas at Austin, Texas, 1968 (unpublished).

⁸ G. R. Satchler, R. M. Drisko, and R. H. Bassel, Phys. Rev. **136**, B637 (1964).

code NEPTUNE⁹ by Tamura, was used for the calculation of theoretical proton partial widths $\Gamma_{l_i}(\text{theor})$. Code GPMAIN uses the same potential as code JULIUS, except that only the spin-orbit and real central terms are employed.

In the analysis of $^{208}\text{Pb}(p, p)$ elastic scattering data,² an optical potential V_n was found which reproduced the binding energies of the $g_{9/2}$, $s_{1/2}$, $g_{7/2}$, and $d_{3/2}$ parent analog states in ^{209}Pb . The depth and geometry of the real part of the proton potential used in the scattering matrix were therefore fixed in accordance with the neutron potential and symmetry term. The imaginary optical parameters were then adjusted to fit the background scattering.

Compared with the case of ^{208}Pb , which has a doubly magic core, the case of ^{136}Xe , with a closed neutron core only, is more complex. Analysis of $^{136}\text{Xe}(d, p)$ ^{137}Xe data has shown that there is rather large fractionation of the $p_{3/2}$, $p_{1/2}$, $h_{9/2}$, and $f_{5/2}$ neutron strengths,^{4,5} and consequently, the neutron potential of the nC system can only be fixed approximately. In addition, the $f_{7/2}$ ground state of ^{137}Xe , the only observed $f_{7/2}$ state, has a (d, p) spectroscopic factor of only approximately 0.70, indicating that ^{136}Xe may not be a good core nucleus. As further evidence of this, the first excited state of ^{136}Xe , a 2^+ collective state at 1.30-MeV excitation, resonates strongly at the low-lying analog resonances,¹⁰ indicating a substantial component of the 2^+ configuration in the parent analog state.

In the present analysis, the $^{136}\text{Xe}(p, p)$ elastic scattering excitation functions were first fitted by means of code JULIUS.⁷ The proton optical parameters were varied to fit the background scattering, and the resonance parameters, namely, the proton partial width $\Gamma_{l_i}^{(\text{A})}$, total width Γ , the resonance energy E_R , and the level shift function Δ_{l_i} , were adjusted to give optimum agreement between the experimental data and the calculated excitation functions. An energy-dependent real proton potential was used, $V = 64 - 0.5E$ (MeV), since energy dependence was found to improve the fit slightly.¹¹

In order to calculate $\Gamma_{l_i}(\text{theor})$, approximate energies of the $f_{7/2}$, $p_{3/2}$, $s_{1/2}$, and $f_{5/2}$ single-particle levels in ^{137}Xe were deduced from the $^{136}\text{Xe}(d, p)$ ^{137}Xe analysis.⁵ These were found to be 0.00, 1.12, 1.67, and 1.77 MeV, respectively. The bound-state well depths were then searched to give the correct binding energies, holding the same geometry, $R = 1.23A^{1/3}$ and $a = 0.66$ F, for the nC system as had been used for the pC system. The well depths so obtained were 47.99, 48.35, 48.68, and 48.49 MeV, respectively. That is, it was not possible

⁹ T. Tamura (to be published).

¹⁰ P. J. Riley, C. M. Jones, J. L. Foster, M. D. Mancusi, and S. T. Thornton, Bull. Am. Phys. Soc. **12**, 565 (1967).

¹¹ The proton optical parameters used were as follows:

$$\begin{aligned} V &= 64.0 - 0.5E \text{ (MeV)}, & r_0 &= 1.23, & a_r &= 0.66, \\ W_d &= 9.4 \text{ MeV}, & r_{0i} &= 1.23, & a_i &= 0.66, \\ V_{\text{so}} &= 5.5 \text{ MeV}, & r_{\text{so}} &= 1.23, & a_{\text{so}} &= 0.66. \end{aligned}$$

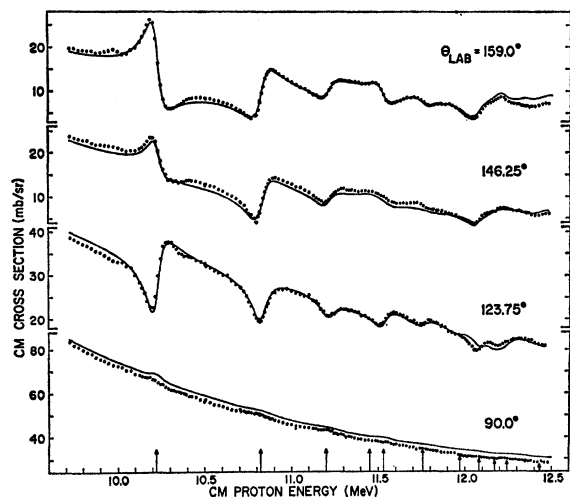


FIG. 3. Theoretical fits to $^{136}\text{Xe}(p, p)$ elastic scattering data at c.m. proton energies between 9.70 and 12.50 MeV. The arrows indicate the resonance energies determined from the analysis.

to obtain a truly unique central potential V_n which reproduced the experimental separation energies of the parent analog states.

The theoretical proton partial widths were then calculated using code GPMMAIN. The appropriate neutron well depths given above were used in the calculation of φ_{nA} . The proton real well depth V_p used in the calculation of χ_{pC} was related to the neutron well depth V_n through $V_p = V_n + 10.7$ MeV, corresponding to a symmetry term $\frac{1}{2}(T_0 V_1) = 26(N-Z)/A$ in the proton potential. V_p thus corresponds very closely to the average depth of the proton potential obtained from the fitting of the excitation functions with JULIUS. Finally, the spectroscopic factors were evaluated using

$$S_{pp} = \Gamma_{l_j}^{(A)} / \Gamma_{l_j}(\text{theor}).$$

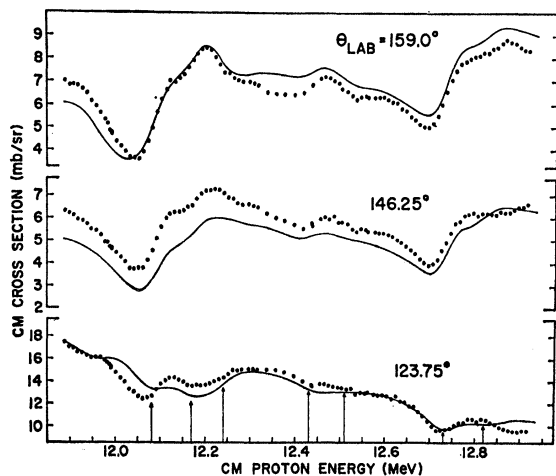


FIG. 4. Theoretical fits to the $^{136}\text{Xe}(p, p)$ elastic scattering data at c.m. proton energies between 11.89 and 12.94 MeV. The arrows indicate the resonance energies determined from the analysis.

It should be noted that two sets of proton optical parameters were found which gave equally good fits to the data.¹² The deduced spectroscopic factors, however, were the same for both sets of parameters.

IV. RESULTS AND DISCUSSION

Fits to the experimental data were made in two overlapping sections; 9.70–12.50 MeV and 11.89–12.94 MeV, corresponding to the two overlapping data sets. These, and all proton energies in this section, are in the c.m. system. The theoretical fits obtained are shown in Figs. 3 and 4. The fits of the lower energy region are in excellent agreement with the data. Slight anomalies in the neighborhood of 9.9 and 10.3 MeV can be attributed to analog resonances in the elastic scattering of protons

TABLE I. Resonance parameters and spectroscopic factors determined from the theoretical fits to the $^{136}\text{Xe}(p, p)$ elastic scattering data. $\Gamma_{l_j}^{(A)}$ is the partial proton width of the resonance and Γ_{l_j} is the total width. Quantities enclosed in parentheses are probable but not certain assignments.

$E_R^{\text{c.m.}}$ (keV)	l_j'	$\Gamma_{l_j}^{(A)}$ (keV)	Γ_{l_j} (keV)	S_{pp}
10 195	$f_{7/2}$	21.5	88.6	0.73
10 794	$p_{3/2}$	37.0	116.0	0.40
11 173	$p_{1/2}$	27.0	111.3	0.27
11 421	$h_{9/2}$	(2.0)	(100.0)	
11 498	$f_{5/2}$	13.0	104.7	0.26
11 724	$f_{5/2}$	8.0	115.0	0.15
11 940	$f_{5/2}$	6.0	115.0	(0.11)
12 050	$p_{(3/2)}$	17.0	117.0	(0.18)
12 140	$p_{(1/2)}$	20.0	117.0	(0.20)
12 209	$f_{(5/2)}$	6.0	110.0	(0.10)
12 399	$p_{(1/2)}$	(6.0)	(100.0)	(0.06)
12 479	$f_{(5/2)}$	(2.0)	(100.0)	(0.03)
12 698	$p_{(3/2)}$	(15.0)	(110.0)	(0.15)
12 788	$p_{(1/2)}$	(8.0)	(100.0)	(0.08)

from ^{134}Xe , which was present as an 8% contamination of the target gas. The effect of the $h_{9/2}$ resonance at 11.421 MeV is visible in the data only at 159°, where it causes a slight dip. This resonance was included in the fit only because the parent analog state was clearly seen in the (d, p) measurements.⁵ At higher energies, the resonances begin to overlap, making accurate determinations of $\Gamma_{l_j}^{(A)}$ very difficult. Hence, extraction of resonance energies and l values was the main purpose of the fit for this energy region, and the deduced spectroscopic factors must be considered to be only approximate.

¹² The second set of proton optical parameters were as follows:

$$\begin{aligned} V &= 64.0 - 0.5E \text{ (MeV)}, & r_{0r} &= 1.24, & a_r &= 0.64, \\ W_d &= 9.4 \text{ MeV}, & r_{0i} &= 1.23, & a_i &= 0.64, \\ V_{s0} &= 5.5 \text{ MeV}, & r_{s0} &= 1.24, & a_{s0} &= 0.64. \end{aligned}$$

TABLE II. A comparison of the $^{136}\text{Xe}(p, p)$ and $^{136}\text{Xe}(d, p)$ analyses. The column labeled δ gives the differences, in keV, between the c.m. proton elastic scattering resonance energies minus 10.195 MeV and the excitation energies of the parent analog states observed in the (d, p) work.

$E_R^{\text{c.m.}}$ (MeV)	$^{136}\text{Xe}(p, p_0)^{136}\text{Xe}$				E^* (MeV)	$^{136}\text{Xe}(d, p)^{137}\text{Xe}^a$				δ (keV)
	$E_R^{\text{c.m.}}$ 10.195	l	j	S_{pp}		l	j	S_{dp}		
10.195	0.00	3	$\frac{7}{2}$	0.73	0.00	3	$\frac{7}{2}$	0.68	0	
10.794	0.60	1	$\frac{3}{2}$	0.40	0.55	1	$\frac{3}{2}$	0.49	50	
11.173	0.98	1	$\frac{1}{2}$	0.27	0.91	1	$\frac{1}{2}$	0.34	70	
11.421	1.23	5	$\frac{3}{2}$		1.12	5	$\frac{3}{2}$	0.31	110	
11.498	1.30	3	$\frac{5}{2}$	0.26	1.20	3	$\frac{5}{2}$	0.24	100	
11.724	1.53	3	$\frac{5}{2}$	0.15	1.41	3	$\frac{5}{2}$	0.16	120	
11.940	1.74	3	$(\frac{5}{2})$	(0.11)	1.61				130	
12.050	1.86	1	$(\frac{3}{2})$	(0.18)	1.70				160	
12.140	1.94	1	$(\frac{1}{2})$	(0.20)						
12.209	2.01	3	$(\frac{5}{2})$	(0.10)	1.84				170	
					1.93					
12.399	2.20	1	$(\frac{1}{2})$	(0.06)	2.03				170	
12.479	2.28	3	$(\frac{5}{2})$	(0.03)	2.11				170	
					2.17					
12.698	2.50	1	$(\frac{3}{2})$	(0.15)	2.30	1	$(\frac{1}{2})$	0.35 ^b	200	
12.788	2.59	1	$(\frac{1}{2})$	(0.08)	2.43	(1)	$(\frac{3}{2})$	0.22	160	
					2.62	(1)	$(\frac{1}{2})$	0.04		
					2.73	(3)	$(\frac{3}{2})$	0.21		
					2.92					
					3.03					
					3.20					

^a See Ref. 5. ^b $S_{dp} = 0.18$ for $J = \frac{3}{2}$.

Resonance parameters and spectroscopic factors determined from the fits are shown in Table I. The spin of the ground-state $f_{7/2}$ analog resonance, and of the low-lying $p_{3/2}$, $p_{1/2}$, $f_{5/2}$, and $f_{3/2}$ analog resonances at energies of 10.195, 10.794, 11.173, 11.498, and 11.724 MeV, respectively, can be considered known on the basis of polarization measurements of proton elastic scattering at analog resonances in ^{139}La by Veaser *et al.*¹³ The spin of the $h_{9/2}$ resonance at 11.421 MeV follows from the conventional shell-model ordering of states. The spin of the higher isobaric analog resonances are somewhat less certain, although the l -value assignments are believed to be correct. The $l=3$ isobaric analog resonances at 11.940, 12.209, and 12.479 MeV have been tentatively assigned spins of $\frac{5}{2}^-$, since the sum rule for the spectroscopic factors, $\sum S_i^{(J)} = 1$, is not exceeded. However, the $^{136}\text{Xe}(d, p)^{137}\text{Xe}$ measurements⁵ indicated the presence of an $l=3$ state with an $f_{5/2}$ spectroscopic factor of 0.21 at an excitation of 2.73 MeV, above the region of the present work. The inclusion of this state would nearly satisfy the sum rule for $f_{5/2}$ states.

Five $l=1$ resonances were observed at proton energies

¹³ L. Veaser, J. Ellis, and W. Haeberli, Phys. Rev. Letters **18**, 1063 (1967).

between 12 and 13 MeV. One additional weak $l=1$ parent analog state was observed in the (d, p) work at an excitation of 2.62 MeV, above the region of the present work. The (d, p) measurements⁵ indicated that some of the $l=1$ states are $p_{3/2}$ states, since otherwise the sum rule would be exceeded for $J = \frac{1}{2}$. In the fits to the two sets of closely spaced $l=1$ resonances (12.050, 12.140, 12.698, and 12.788 MeV), the only assumed spins which allowed a reasonable fit to the elastic scattering data were $\frac{3}{2}$ for the 12.050- and 12.698-MeV resonances, and $\frac{1}{2}$ for the 12.140- and 12.788-MeV resonances. All other assumed spin values resulted in a deterioration of the theoretical fits. The fitting of these two states with $p_{3/2}$ spin assignments is therefore suggestive that their spins are $\frac{3}{2}$. With the assumed $l=1$ spin values as indicated in Table I, the sums of the spectroscopic factors for $p_{1/2}$ and $p_{3/2}$ states are 0.61 and 0.73, respectively. Using the $p_{1/2}$ spectroscopic factor deduced from the (d, p) work of 0.04 for the state at an excitation of 2.62 MeV, the sum of the spectroscopic factors for $p_{1/2}$ states is 0.65. The sum rule is therefore apparently nearly satisfied both for $p_{3/2}$ and for $p_{1/2}$ states.

A detailed comparison of the present work with the

TABLE III. A comparison of spectroscopic factors obtained in the $^{136}\text{Xe}(p, p)$ and $^{136}\text{Xe}(d, p)$ analyses. The column $S_{dp}(a)$ gives spectroscopic factors obtained in the work of Moore *et al.*^a The column $S_{dp}(b)$ gives spectroscopic factors obtained using the optical parameters^b that were used to fit the proton elastic scattering data.

State	$E_R^{c.m.}$ (MeV)	S_{pp}	$S_{dp}(a)$	$S_{dp}(b)$
$f_{7/2}$	10 195	0.73	0.68	0.77
$p_{3/2}$	10 794	0.40	0.49	0.56
$p_{1/2}$	11 173	0.27	0.34	0.38
$f_{5/2}$	11 498	0.26	0.24	0.28
$f_{3/2}$	11 724	0.15	0.16	0.18
$p_{3/2}$	12 050	(0.11)		
$p_{1/2}$	12 140	(0.20)		
$f_{5/2}$	12 209	(0.10)		

^a Reference 5; the optical parameters used were those of Ref. 14.

^b Listed in Ref. 11.

$^{136}\text{Xe}(d, p)$ ^{137}Xe 5 analysis is shown in Table II. On the whole, there is excellent agreement between the two experiments. The parent analog of the resonance observed in the elastic scattering at 12.140 MeV was not observed in the (d, p) work, probably because of the presence of the deuteron elastic scattering peak in the (d, p) spectrum. In the (p, p) work, l -value assignments and approximate spectroscopic factors have been deduced for the resonances at 11.940, 12.050, 12.209, 12.399, and 12.479 MeV. Because of the presence of the deuteron elastic scattering peak in the spectra, neither l -value assignments nor spectroscopic factors could be evaluated for the parent analogs of these states in the (d, p) work. The analogs of the weak states at excitations of 1.93 and 2.17 MeV in the (d, p) work were not observed in the elastic scattering measurements, either because of the low spectroscopic factors associated with the states, or because they correspond to rather high orbital angular momentum transitions. The $p_{1/2}$ spectroscopic factor of 0.08 deduced for the resonance at 12.788 MeV is in disagreement with the value of 0.22 obtained in the (d, p) work for the parent state.

As a check on the proton optical parameters determined using code JULIUS, and as a further comparison between the (d, p) and (p, p) analysis, the (d, p) data, previously analyzed⁵ using Perey's average optical parameters,¹⁴ were reanalyzed using the same proton

¹⁴ The proton optical parameters used were as follows:

$$\begin{aligned} V &= 57.06 \text{ MeV}, & r_{0r} &= 1.25, & a_r &= 0.65, \\ W_d &= 11.64 \text{ MeV}, & r_{0i} &= 1.25, & a_i &= 0.47, \\ V_{so} &= 7.50 \text{ MeV}, & r_{so} &= 1.25, & a_{so} &= 0.65. \end{aligned}$$

optical parameters that were used to fit the elastic scattering data. Table III shows a comparison of spectroscopic factors obtained. The results show reasonable agreement, although it is clear, and to be expected, that the use of the same proton optical parameters in the (d, p) and the (p, p) analyses does not necessarily improve the agreement of the spectroscopic factors. The spectroscopic factors obtained from the (d, p) work using the new proton parameters are consistently higher than those obtained in the (p, p) work, with the most serious discrepancies arising for the $l=1$ states.

As pointed out in Ref. 2, the calculated partial width depends to some extent on the geometry of the bound-state potential chosen to describe the parent analog state, and particularly on the radius parameter r_{0r} . Therefore, any ambiguity in potential might be expected to cause an uncertainty in S_{pp} , just as it does in the distorted-wave Born analysis (DWBA) of (d, p) data, as has been indicated in Table III. In the present work, the dependence of the spectroscopic factors on the radius parameter r_{0r} and on the diffuseness a_r has been studied in some detail. As r_{0r} is varied, it has been found necessary, in order to maintain a good fit to the elastic scattering data, to vary the diffuseness a_r in such a way that the change in the spectroscopic factor is negligible. That is, good fits to the elastic scattering data can only be obtained for a certain range of r_{0r} and a_r , all of which predict approximately the same results for S_{pp} . Figure 5 shows S_{pp} for different values of r_{0r} , plotted as a function of the diffuseness a_r for the five lowest isobaric analog resonances. The dots indicate the value of a_r for a given value of r_{0r} for which the best fits to the data were obtained without changing the imaginary optical well. The solid lines, where drawn, indicate the range of a_r for a given value of r_{0r} for which good fits to the data could be obtained by suitable adjustment of the imaginary terms of the optical potential. All points along the solid lines predict approximately the same value of spectroscopic factor; therefore, the over-all uncertainty in S_{pp} for a given analog resonance is surprisingly small. The variation in S_{pp} for different values of optical potential is seen to be largest for the ground-state $f_{7/2}$ resonance.

In the extraction of spectroscopic factors, the neutron well depths were searched to give the correct binding energies. The effect of this procedure on the spectroscopic factors was checked by choosing an average well depth of 48.376 MeV (average of $f_{7/2}$, $p_{3/2}$, $p_{1/2}$, and $f_{5/2}$ well depths) and searching for the binding energies using code GPMAN. The only significant effect of the procedure was to increase the spectroscopic factor of the ground-state $f_{7/2}$ resonance from 0.74 to 0.76. The use of a 47.988-MeV well depth, the calculated $f_{7/2}$ well depth, changed the spectroscopic factors of the remaining states by less than 2%.

In the analysis, the level shift function Δ_l was

treated as a variable parameter. For all but the lowest two analog resonances, the $f_{7/2}$ and $p_{3/2}$ resonances, this parameter was taken to be zero. For the $f_{7/2}$ and $p_{3/2}$ resonances, it was necessary to use negative values of Δ_{l_i} to obtain good fits to the data. This is indicated by Fig. 6, which shows three fits to the 159° data between 9.7 and 12.5 MeV. The three curves, one for negative

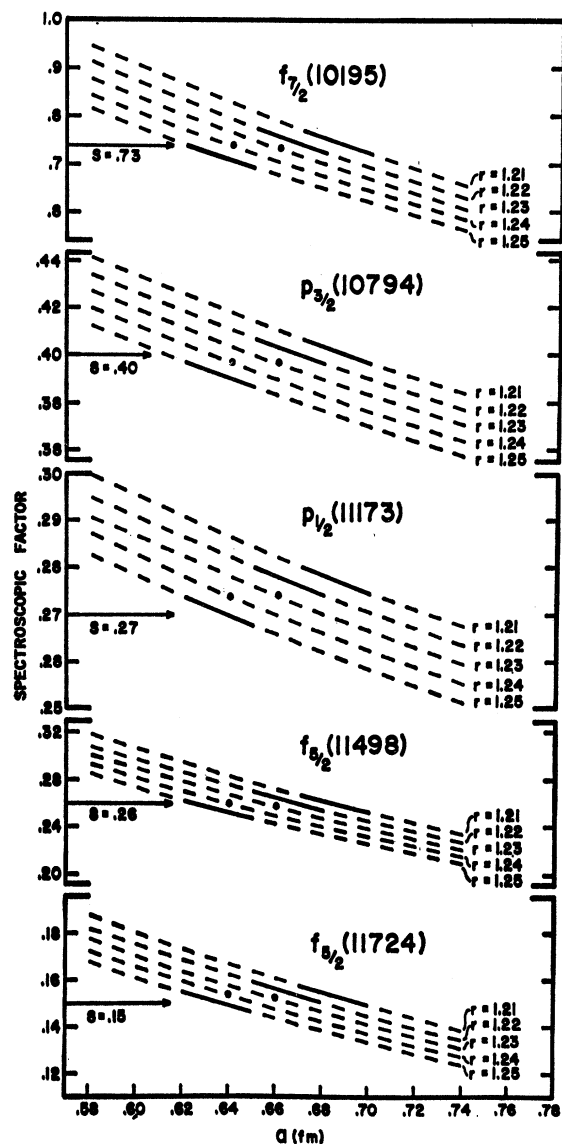


FIG. 5. Spectroscopic factor S_{pp} plotted versus diffuseness a_r for different values of the radius r_{0r} for the lowest five isobaric analog resonances in ^{137}Cs . The solid lines indicate the range of a for which good fits could be obtained. The dots indicate the value of a_r for a given value of r_{0r} for which the best fits to the data were obtained without changing the imaginary optical well. The value of S_{pp} quoted is indicated at the left of the figure.

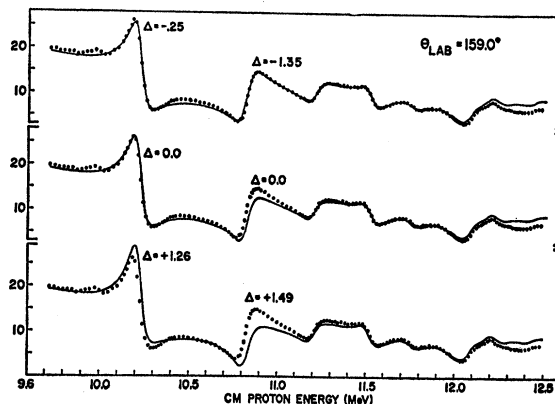


FIG. 6. Theoretical fits to the elastic scattering data between 9.70 and 12.50 MeV at a scattering angle of 159.0° , showing the effect of variation in the parameter Δ_{l_i} .

values, one for zero values, and one for positive values, demonstrate a deterioration of the fit as Δ_{l_i} becomes more positive. Clearly, the values in the upper curve give the best fit.

The Coulomb displacement energy ΔE_C , between the analog and the parent state, is given by the relationship $\Delta E_C = E_p + Q_{dp} + 2.225$ MeV, where E_p is the c.m. proton energy at which the analog resonance in the nucleus $(N, Z+1)$ occurs, Q_{dp} is the (d, p) reaction Q value, and 2.225 MeV is the deuteron binding energy. A value of 1.637 ± 0.020 MeV was used for the (d, p) reaction Q value.⁵ The resulting Coulomb displacement energy is 14.057 ± 0.040 MeV, in fair agreement with the value of 14.120 ± 0.060 MeV predicted by the empirical relationship of Long *et al.*¹⁵

$$\Delta E_C = B_1 + B_2 Z(A)^{-1/3},$$

where $B_p = (0.849 \pm 0.029)$ MeV, $B_2 = (1.429 \pm 0.003)$ MeV; Z and A are the charge and mass numbers for the parent analog nucleus.

ACKNOWLEDGMENTS

The data reported in this work were measured at Oak Ridge National Laboratory, and we wish to thank the members of the laboratory for their cooperation and help during the experiment. The authors are deeply indebted to Dr. S. A. A. Zaidi for helpful discussions and assistance in carrying out the analysis. One of us (P. A. M.) gratefully acknowledges financial support from an Atomic Energy Commission Special Fellowship in Nuclear Science and Engineering.

¹⁵ D. D. Long, P. Richard, C. F. Moore, and J. D. Fox, *Phys. Rev.* **149**, 906 (1966).